

Motifs within the CLN3 protein: modulation of cell growth rates and apoptosis

Dixie-Ann N. W. Persaud-Sawin^{1,2}, Antonius VanDongen³ and Rose-Mary N. Boustany^{1,2,*}

¹University Program in Genetics, ²Departments of Pediatrics and Neurobiology and ³Department of Pharmacology, Duke University Medical Center, Durham, NC, 27710, USA

Received April 26, 2002; Revised June 27, 2002; Accepted June 28, 2002

Juvenile Batten disease (JNCL) is an autosomal recessive disease that results from mutations in the *CLN3* gene. The wild-type *CLN3* gene coding sequence has 15 exons, and the translated protein consists of 438 amino acids. The most commonly observed mutation is a 1.02 kb deletion in the genomic DNA. This deletion results in a truncated protein due to the loss of amino acids 154–438, and the introduction of 28 novel amino acids at the c-terminus. We demonstrate that, compared to normal controls, *CLN3*-deficient immortalization of lymphoblasts homozygous for this deletion grow at a slower rate, and show increased sensitivity to etoposide-induced apoptosis, supporting the notion that *CLN3* may negatively regulate apoptosis. Using immortalized JNCL lymphoblast cell lines as a model system, we assess the effects of specific *CLN3* mutations on cell growth rates and protection from etoposide-induced apoptosis. Protection from etoposide-induced apoptosis occurs and the cell growth rate is restored following transfection of JNCL lymphoblasts with mutant *CLN3* cDNA that includes exons 11 or 13. We show that deletion of the glycosylation sites 71NQSH74 and 310NTSL313, and also mutations within the highly conserved amino acid stretches 184WSSGTGGAGLLG195, 291VYFAE295 and 330VFASRSSL337, result in slowed growth and susceptibility to apoptosis.

INTRODUCTION

Batten disease is a collective term for a group of diseases known as the neuronal ceroid lipofuscinoses (NCLs). Batten disease is one of the most common neurodegenerative disorders of childhood, with an incidence of 1 in 100 000 in the general population (1). JNCL, or the juvenile-onset form of NCL (OMIM 204200), is caused by mutations within the *CLN3* gene, and is an autosomal recessive disease (2). The age of onset is usually 4–10 years, with the first manifestations being rapid loss of vision due to retinitis pigmentosa. Clinical hallmarks are seizures, psychomotor and cognitive decline, blindness, and death, commonly in the mid-20s to late 20s (2,3).

The pathology of JNCL is remarkable for massive neuronal death, photoreceptor loss and the accumulation of lipopigments in lysosomes (4,5). Autofluorescent bodies and fingerprint profiles within cells are widespread in JNCL brain tissue, especially within the surviving pyramidal neurons of the hippocampal sectors CA2–CA4 (5,6). These bodies consist mainly of subunit *c* or 9 of mitochondrial ATP synthase (5–8).

Other NCL genes include *CLN1*, *CLN2*, *CLN5*, *CLN6* and *CLN8*. *CLN1* and *CLN2* code for palmitoyl-protein thioesterase 1 (PPT1) and for the lysosomal protease tripeptidyl peptidase 1

(TPP1), respectively (9,10). *CLN3* (11), *CLN5* (12), *CLN6* (13) and *CLN8* (14) most likely are transmembrane proteins. The hydropathy profile for *CLN3* suggests that it has 5–11 transmembrane domains (11). There is some controversy concerning the location of the *CLN3* protein. Different studies have localized the *CLN3* protein to the cell membrane (15), the lysosomal membrane in non-neural tissues (16,17), the mitochondria in retinal cells (18) and the Golgi apparatus (19). *CLN3* has been shown to be abundantly expressed in primary rat neurons, rat neuronal tissue and synaptosomes, with exclusion, however, from both lysosomes and synaptic vesicles (20,21). The different conclusions reached in these studies suggest that the true location or locations of *CLN3* may be species and/or tissue specific.

We have previously claimed that *CLN3* may have anti-apoptotic properties (22,23). This claim has been supported by findings based on electron microscopy and TUNEL assay in *CLN3*-deficient human brain (24). Increased apoptosis in *CLN3*-deficient or JNCL patient leukocytes has been documented by others (25). Previous studies have demonstrated that overexpression of *CLN3* enhances growth of NT2 cells, and protects from apoptosis induced by chemotherapeutic drugs and serum starvation (22). *CLN3* is developmentally regulated (26). It is also upregulated in a number of human and mouse

*To whom correspondence should be addressed at: Duke University Medical Center, MSRB Box 2604, Research Drive, Durham, NC, 27710, USA. Tel: +1 9196816220; Fax: +1 9196818090; Email: boust001@mc.duke.edu

cancer cell lines and solid human colon cancer. Blocking of CLN3 expression in human cancer cells has led to inhibition of cancer cell growth and to increased apoptosis (27). Blocking of CLN3 expression in human differentiated, postmitotic hNT neurons results in spontaneous and unprovoked apoptosis (23). Yeast knockout models have suggested that CLN3 is involved in pH regulation (28,29). There is evidence to suggest that the onset of apoptosis is characterized by an initial alkalinization of the mitochondrial matrix, followed by cytosolic acidification and cell death (30).

The *CLN3* gene is highly conserved across species. Homologs for *CLN3* in the dog, mouse, *Caenorhabditis elegans* and yeast bear 78%, 75%, 37% and 34% identity to the human *CLN3* gene, respectively (22). This underscores the biological importance of CLN3. CLN3 is a novel protein with stretches of conserved amino acids along its length, including residues 184WSSGTGGAGLLG195, 291VYFAE295 and 330VFASRSSL337. We hypothesized that the apoptosis-modulating activity of CLN3 could be defined by stretches of amino acids within these conserved regions.

There are 31 mutations known to cause JNCL (31–33). Eighty five per cent of the cases are due to a 1.02 kb deletion in the genomic DNA (2), while the other 15% result from point or frameshift mutations. Lymphoblasts derived from patients homozygous for this deletion grow more slowly than normal controls, and show increased sensitivity to etoposide-induced apoptosis. We address the following questions: (1) Do specific mutations create a cell phenotype similar to that observed in JNCL cell lines derived from patients homozygous for the 1.02 kb deletion? (2) Do these mutations reside within highly conserved regions of CLN3? (3) Does the elimination of potentially important biological sites within the CLN3 protein affect cell growth rates and apoptosis? (4) Does altering the charge and/or hydrophobicity of specific amino acids within CLN3 affect growth and apoptosis of cells? We present data that support the notion that CLN3 may regulate apoptosis, and that many but not all of the elements responsible for this regulation reside at the c-terminus of the CLN3 protein.

RESULTS

Slowed growth rate of JNCL patient lymphoblasts

Our results indicate that untransfected CLN3-deficient cells derived from patients homozygous for the common deletion show reduced growth rates when compared to normal untransfected lymphoblasts, and the *P*-value is <0.05 (Fig. 1A). We also show that untransfected immortalized JNCL lymphoblast cell lines derived from four different patients harboring the 1.02 kb deletion show similar growth rates ($P > 0.05$). The introduction of *CLN3* by transfection into these JNCL patient lymphoblasts reverses this growth rate defect when compared to transfection with an empty vector control (Fig. 1B) ($P < 0.05$). Notably, JNCL patient cells show an increased rate of cell death compared to normal lymphoblasts, with a *P* value of <0.05 (Fig. 1C). A reversal in the rate of death is accomplished following transfection with a *CLN3*-bearing plasmid ($P > 0.05$). Maximum CLN3 expression is

observed between time points 0 and 48 h, after which it declines.

The CLN3 protein does not affect DNA synthesis

Rates of thymidine incorporation into DNA by JNCL lymphoblasts were compared following transfection with an empty vector control or a *CLN3* cDNA construct. Rates for JNCL lymphoblasts transfected with either an empty vector control or wild-type *CLN3* cDNA are shown in Figure 1D. The rates of thymidine incorporation show no significant differences, and the *P*-value is >0.5 . We also compared the rate of thymidine incorporation for deletion constructs containing *CLN3* exons 1–4, 1–7, 1–8, 1–9, 1–10, 1–11, 1–12, 1–13, 1–14 and 1–15. The effect of the *CLN3* deletion construct harboring exons 1–4 of the *CLN3* cDNA on thymidine incorporation is shown in Figure 1D. There are no significant differences in the rates of thymidine incorporation among any of the generated deletion constructs, and the *P*-value for all points was >0.5 . This suggests that the effect of CLN3 on the cell growth rate is not due to differences in the rate of DNA synthesis, but due to increased cell death in patient cell lines (Fig. 1C).

Increased etoposide-induced apoptosis in JNCL patient lymphoblasts

Immortalized JNCL lymphoblasts homozygous for the common deletion were transfected with either an empty vector control or the full *CLN3* cDNA, treated with etoposide and then analyzed using the TUNEL assay. JNCL lymphoblasts transfected with the full *CLN3* cDNA (Fig. 2C and D) show more protection from etoposide-induced apoptosis than is observed in JNCL lymphoblasts transfected with an empty vector (Fig. 2A and B), with a *P*-value of <0.05 . Our results confirm that deletion of *CLN3* results in increased cell death. Results were corroborated using the JC-1 mitochondrial membrane potential assay (Table 1). The degree of protection is determined by the percentage of live cells after treatment with etoposide divided by the percentage of live cells before treatment with etoposide. Compared to JNCL cells transfected with the empty vector control, JNCL patient lymphoblasts transfected with the full *CLN3* cDNA show significant protection from etoposide-induced apoptosis ($48 \pm 0.8\%$, $P > 0.5$ versus $96 \pm 2.8\%$, $P < 0.005$) (Table 1, Fig. 2). This supports the results of previous studies (20–22).

Effect of exons 11 and 13 of CLN3 on cell growth rates and apoptosis

Our next aim was to determine the regions of the *CLN3* gene that may impact on cell growth rates. We used deletion constructs generated from the conserved 3' end (34), and established growth curves following transfection of the CLN3-deficient cells with each construct. The constructs containing exons 1–13 restore cell growth potential to normal levels as opposed to transfection with the empty vector, and the *P* value is <0.05 (Fig. 3). The effect of transfection of the construct containing exons 1–11 into JNCL patient cells is a significantly enhanced growth rate, as opposed to the effect of the empty vector, and the *P*-value is <0.05 . Inclusion of exon 11 results in

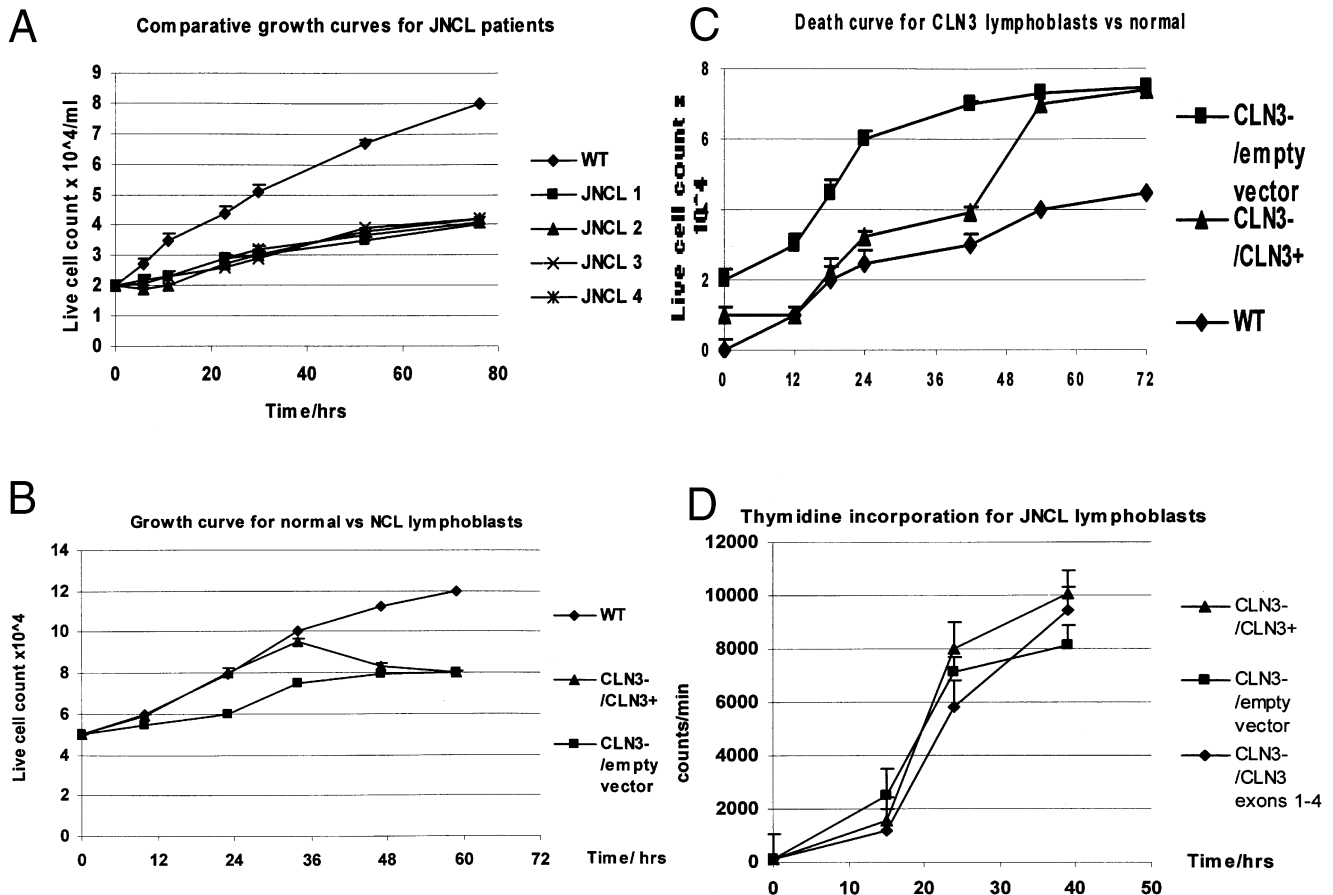


Figure 1. (A) Growth curves of untransfected CLN3-deficient and normal lymphoblast cell lines. Immortalized JNCL cells derived from patients homozygous for the 1.02 kb deletion grow at a diminished rate compared to normal wild-type (WT) lymphoblasts ($P < 0.05$). Untransfected cell lines from different patients (JNCL 1, JNCL 2, JNCL 3, JNCL 4) that are homozygous for the 1.02 kb deletion grow at similar rates ($P > 0.05$). (B) Growth curves comparing immortalized JNCL cell lines transfected with CLN3 cDNA and an empty vector control. Reintroduction of full-length CLN3 cDNA (CLN3-/CLN3+) into JNCL patient cell lines, as opposed to the reintroduction of the empty vector (CLN3-/empty vector), restores the growth potential to normal levels. Levels decline 40 h post-transfection due to declining protein levels. (C) Death curve for CLN3-deficient (JNCL) lymphoblasts. Immortalized JNCL patient cells show a higher death rate than observed in normal lymphoblasts ($P < 0.05$). The reintroduction of full-length CLN3 cDNA (CLN3-/CLN3+) into immortalized JNCL patient cells, as opposed to the reintroduction of the empty vector, lowers the rate of cell death ($P < 0.05$). (D) Thymidine incorporation by immortalized, transfected JNCL cell lines. Deletion of CLN3 exons 1-4 or 1-13 does not affect the rate of thymidine incorporation. CLN3-deficient lymphoblasts incorporate thymidine at a rate similar to normal lymphoblasts ($P < 0.05$). Deletion constructs containing exons 1-7, 1-8, 1-9, 1-10, 1-11, 1-13 and 1-14 of the CLN3 cDNA also gave similar results (data not shown).

a rate of cell growth that is somewhat slower than that observed for JNCL patient cells transfected with the full *CLN3* cDNA, and the P -value is < 0.05 . Both TUNEL and JC-1 analyses demonstrate that the presence of exons 11 and 13 provides transfected JNCL lymphoblasts with protection from etoposide-induced apoptosis, and the degrees of protection observed were 87% and 96%, respectively (raw data not shown; Table 1). *CLN3* constructs lacking exons 11 and 13 fail to confer significant protective properties to JNCL patient lymphoblasts after transfection (Table 1).

Amino acid residues important for the impact of CLN3 on apoptosis

We have shown that inclusion of exons 11 and 13 is necessary for the normalizing effect of the *CLN3* gene on cell growth rates and apoptosis. Three naturally occurring mutations within

exon 11 and 13 are of interest: E295K (exon 11), V330C and R334D (both in exon 13) (31,32).

We introduced changes that could either alter charge and/or hydrophobicity at these specific amino acid sites or keep these parameters similar. The data (Fig. 4A) illustrate that transfection with *CLN3* cDNA harboring mutations at R334 that result in a change of charge from basic to acidic (R334D, R334H, R334C) did not correct growth rate defects and had similar effects to transfection with the empty vector control ($P < 0.05$). However, transfection with the mutant *CLN3* cDNA construct resulting in R334K (changing basic to basic) did restore the cellular growth rate to within normal levels ($P < 0.05$). Transfection with any type of *CLN3* cDNA harboring mutations affecting residues E295 (E295K or E295D) and V330 (V330C or V330L) maintained the slowed JNCL cell growth rate phenotype (Fig. 4B). TUNEL (Fig. 5) and JC-1 (data not shown) staining demonstrate that transfection of

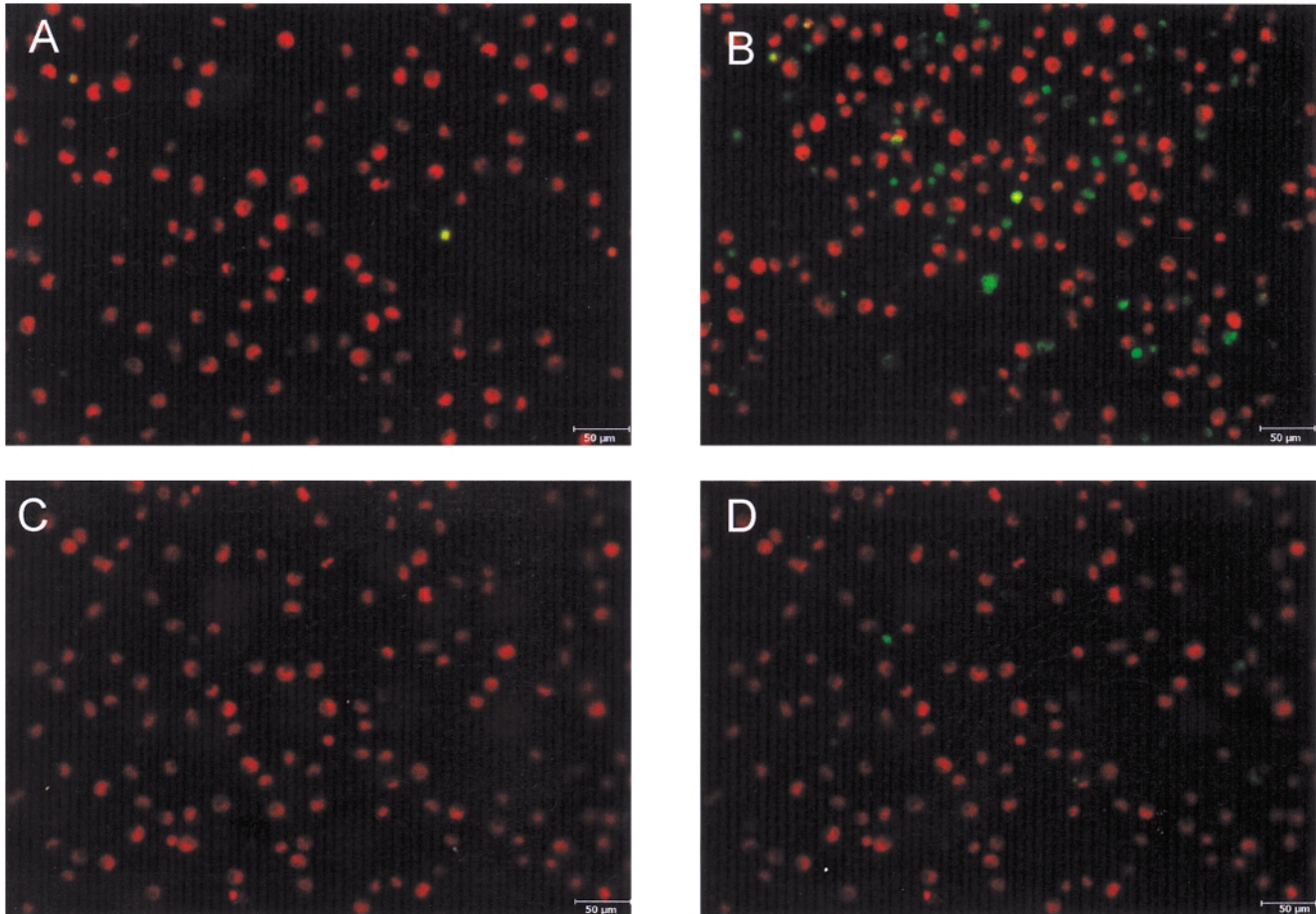


Figure 2. TUNEL staining of immortalized JNCL patient lymphoblasts. (A, B) JNCL cells transfected with an empty vector. (C, D) JNCL lymphoblasts transfected with the full *CLN3* cDNA. (A, C) JNCL cells before treatment with etoposide. (B, D) JNCL cells after treatment with etoposide. The *CLN3* protein provides protection from etoposide-induced apoptotic death ($P < 0.05$). 400 \times magnification, scale bar = 50 μm .

Table 1. Protection from apoptosis of JNCL patient lymphoblasts after transfection with *CLN3* deletion/mutant constructs^a

Transfection	(a) % live cells; no etoposide	(b) % live cells; with etoposide	% protection (b/a)
Empty vector control	30.4	14.7	48 \pm 0.8
<i>CLN3</i> ⁺	80	77	96 \pm 2.8
Exons 1–13	80	76.6	96 \pm 1.4
Exons 1–12	63.3	55	87 \pm 2.8
Exons 1–11	62.5	54	86 \pm 0.7
Exons 1–4	51	29	57 \pm 2.8
E295K	73	24	33 \pm 1.4
V330C	50	32	64 \pm 2.8
R334D	61	27	44 \pm 1.4

^aTransfected cells treated with etoposide were assayed using JC-1 staining. Cells transfected with constructs containing exon 13 show more protection from etoposide-induced apoptosis than cells transfected with the empty vector ($P < 0.005$). Transfection of cells with constructs containing exon 11 gives more protection from etoposide-induced apoptosis than control transfections ($P < 0.005$), but less protection than cells transfected with constructs containing exon 13 ($P < 0.05$). Constructs missing exons 11 and 13 do not provide patient cells with significant protection from etoposide-induced apoptosis when compared to control transfections ($P > 0.05$). These constructs maintained the increased sensitivity to apoptosis of JNCL cells (E295K, V330C, R334D).

immortalized JNCL lymphoblasts with mutant *CLN3* cDNA harboring the mutations R334D, E295K and V330C did not reverse sensitivity to etoposide-induced apoptosis. The percentage protection from etoposide-induced apoptosis observed in cells after transfection with these constructs was similar to that of JNCL cells transfected with the empty vector (Table 1). The mutations E295K, E295D, V330C, V330L, R334D, R334H and R334C were not quantitatively distinguishable from each other ($P > 0.05$).

In 85% of JNCL patients, the block of conserved amino acids 184WSSGTGGAGLLG195 is lost due to the 1.02 kb deletion in genomic DNA. This deletion results in a truncated protein with loss of more than 200 amino acids from the c-terminus (2). A growth phenotype consistent with the one observed in JNCL patient cells is observed following transfection with mutant *CLN3* cDNA that corresponds to this deletion, and the P -value is > 0.05 (Fig. 4C). The residues V330 and R334 form part of a highly conserved stretch of amino acids, 330VFASRSSL337. Mutations affecting this region maintain the deficient cell growth rate phenotype (Fig. 4A and B).

The motif 291VYFAE295 is highly conserved among *CLN3* orthologs, and is homologous to amino acid sequences within the S5 domain of K^+ channels (35), and the amyloid- β precursor

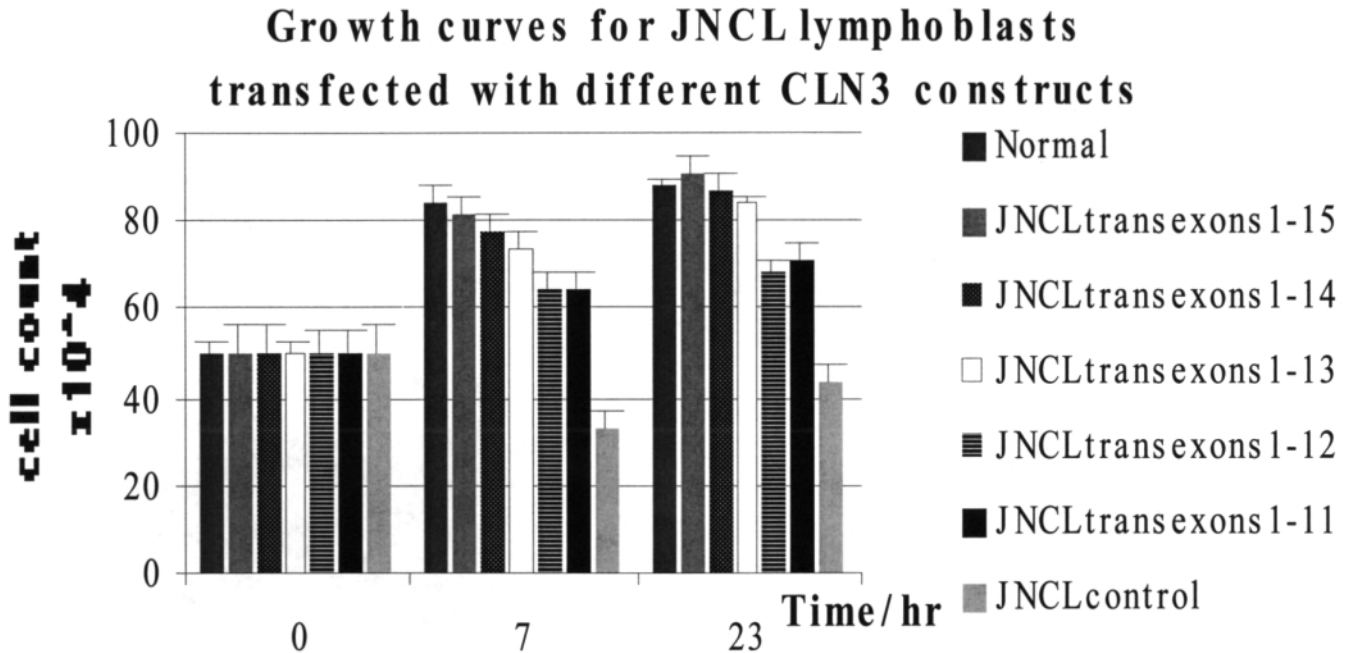


Figure 3. Live cell counts following transfection with CLN3 deletion constructs (exons 1–11, 1–12, 1–13, 1–14 and 1–15). Cell numbers are significantly lower in JNCL cells transfected with the empty vector control compared to JNCL cells transfected with the full-length CLN3 cDNA ($P < 0.05$). The presence of exon 11 and 13 restores growth potential when compared to the empty vector control ($P < 0.05$). The order of the transfected cell lines analyzed for each time point is indicated by the same sequence shown in the key on the right.

peptide 19VFFAE22 (36,37) (<http://www.ncbi.nlm.nih.gov>). We show that constructs resulting in deletion of residues 291VYFAE295 maintain the phenotype of diminished growth, similar to the one seen in JNCL patient lymphoblasts, and the P -value is >0.5 . The mutation resulting in Y292W, located within this stretch of residues, also maintains a reduced growth rate phenotype ($P > 0.05$). However, the CLN3 mutation resulting in Y292F, F being the corresponding residue in normal amyloid- β precursor protein, restores the rate of cell growth to normal, and the P -value is >0.05 (Fig. 4D).

Impact of glycosylation residues 71–74 and 310–313 on cell growth rates

There are four potential glycosylation sites and 12 potential phosphorylation sites within CLN3 (2). It is suggested that the CLN3 protein undergoes post-translational modification by phosphorylation (38,39) and glycosylation (17). CLN3 also harbors potential mitochondrial targeting signal (11) and farnesylation sites (38).

Mutant CLN3 clones affecting each of these sites were individually transfected into JNCL patient lymphoblasts, and growth curves were established for each by the trypan blue dye exclusion assay. Deletion of each of the phosphorylation sites produces a growth curve similar to that established for JNCL patient lymphoblasts transfected with the full-length CLN3 cDNA ($P > 0.05$, data not shown). Deletion of the mitochondrial targeting signal or the farnesylation site did not affect cell growth rate (Fig. 4C; $P > 0.05$). Independent deletion of each of the glycosylation sites corresponding to residues 49NSFY52

and 85NSSS88 did not affect the growth rate ($P > 0.05$, data not shown). Deletion of the DNA sequences corresponding to the glycosylation sites defined by amino acid residues 71NQSH74 results in a similar growth rate pattern to the one observed in JNCL patient lymphoblasts transfected with the empty vector control, and the P -value is >0.05 (Fig. 6A). Deletion of the DNA sequences corresponding to glycosylation sites defined by amino acid residues 310NTSL313 results in a decrease in the growth potential when compared to JNCL patient cells transfected with the full CLN3 cDNA. This decrease was less marked than that observed for the deletion of residues 71NQSH74, and the P -value is <0.05 .

A hydropathy profile created at www.expasy.ch/tools/TMHMM indicates that the CLN3 protein could harbor 5–11 possible transmembrane domains with a putative pore at amino acid residues 299–343 (Fig. 6B). According to this profile, the glycosylation site defined by residues 71NQSH74 is located within the first putative external loop, and the glycosylation site defined by residues 310NTSL313 is within the putative pore of CLN3. Residues V330 and R334 also reside within this pore. The conserved stretch 291VYFAE295 is located in transmembrane domain 7, which lines the putative pore (Fig. 6B).

Levels of CLN3p expression are unaffected following mutation of the CLN3 cDNA

Mutagenesis of cDNA can lead to unstable and easily disrupted nascent protein and erroneous results. Here we show that this is not the case. Western blot analysis (Fig. 7) illustrates that CLN3p is expressed in higher quantities in JNCL lymphoblasts

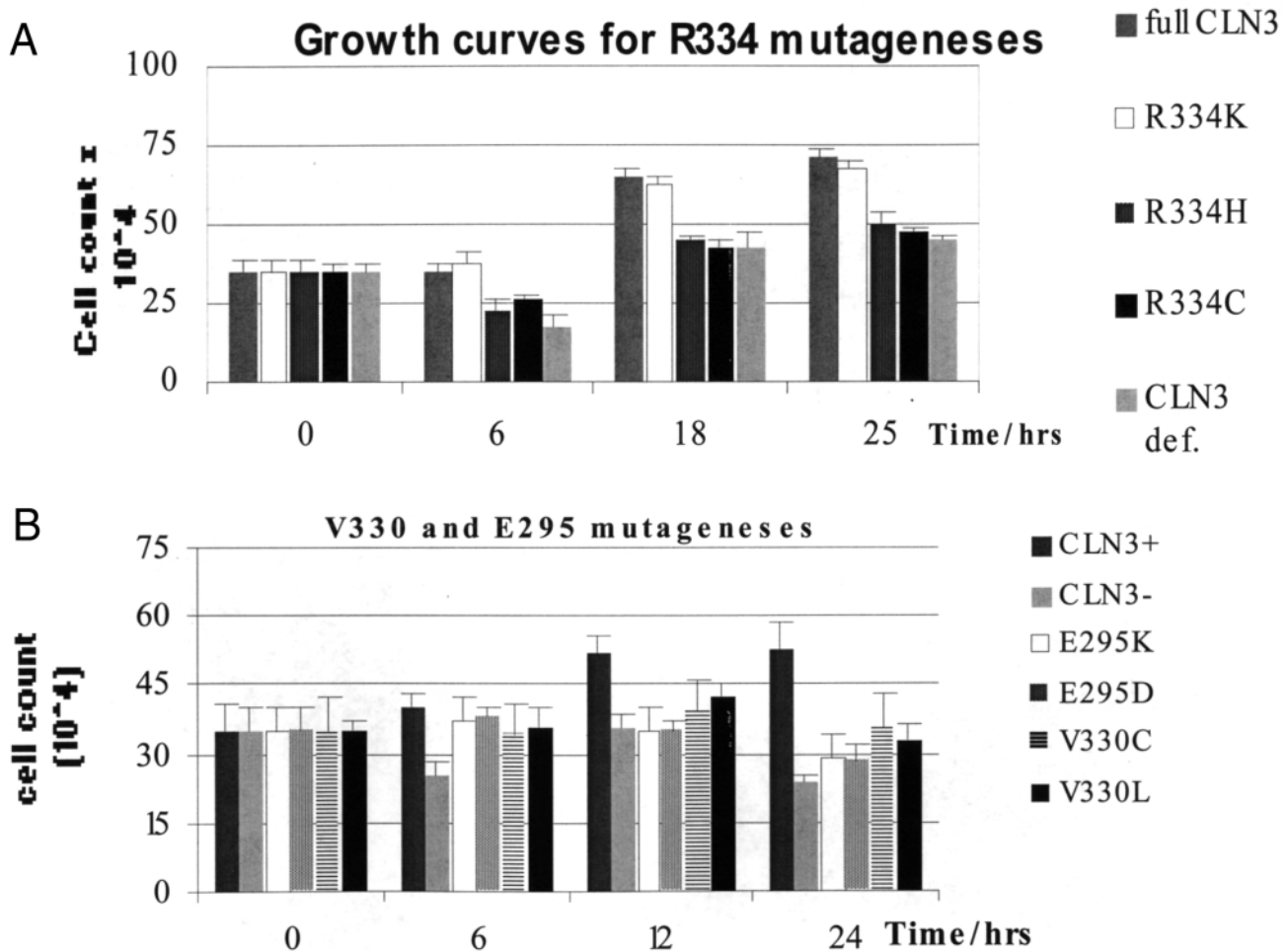


Figure 4. Live cell counts of JNCL lymphoblasts following transfection with *CLN3* mutagenized clones. All cell numbers were established by trypan blue dye exclusion assay. **(A)** Transfection with the R334D, R334C and R334H (not shown) mutant constructs produces effects that are similar to those in the JNCL patient cells transfected with the empty vector, and these were statistically significant ($P > 0.05$). Transfection of JNCL cells with the mutant *CLN3* construct R334K restores the cell numbers to normal levels. Twenty-four hours following transfection, expression of the *CLN3* protein becomes noticeable. There is a decrease in the cell numbers observed between JNCL patient cells transfected with the full *CLN3* cDNA and the mutants R334H, R334D and R334C ($P < 0.05$). **(B)** Mutations E295K and E295D produce similar defects in the growth rate. Mutations at V330 also create a similar phenotype to mutations at E295 and to JNCL patient cell lines transfected with the empty vector control. Mutations at E295 and V330 produce effects similar to each other, and to the empty vector control ($P > 0.05$). The growth rates after transfection with *CLN3* constructs with these mutations are significantly lower than the rate of cell growth for JNCL patient cells transfected with the full *CLN3* cDNA ($P < 0.05$). All mutations result in discernible growth defects. Statistically significant differences are observed between JNCL patient lymphoblasts transfected with the full *CLN3* cDNA and JNCL patient lymphoblasts transfected with *CLN3* cDNA harboring the E295, V330 and R334 *CLN3* mutations ($P < 0.05$). **(C)** Deletion of the conserved region 184WSSGTGGAGLLG195 creates a growth phenotype similar to that of JNCL patient cells transfected with the empty vector control ($P > 0.05$). Deletion of the farnesylation site does not affect the growth rate. **(D)** Deletion of the highly conserved region 291VYFAE295 creates a similar growth phenotype to JNCL patient cells ($P > 0.05$). The mutation Y292W results in a similar growth phenotype to that observed when there is a deletion of 291VYFAE295 ($P > 0.05$). The mutation Y292F does not alter the growth rate significantly when compared to transfection with the full *CLN3* cDNA ($P > 0.05$), but this rate is statistically different from the growth rate of cells transfected with the empty vector ($P < 0.01$). The order of the transfected cell lines analyzed for each time point is indicated by the same sequence shown in the key on the right.

transfected with either wild-type or mutated *CLN3* cDNA than in JNCL lymphoblasts transfected with the empty vector control. We also show that *CLN3p* is expressed at similar levels in JNCL lymphoblasts transfected with either wild-type *CLN3* cDNA or mutated *CLN3* cDNA. The results also confirm the transient effect of *CLN3p* 50 h post-transfection. We show by growth curve analysis and western blot that the *CLN3* protein levels start to decline 48–50 h following transfection with *CLN3* cDNA.

DISCUSSION

Immortalized *CLN3*-deficient lymphoblasts derived from patients homozygous for the common 1.02 kb deletion were used as the assay model system for testing the effect of various *CLN3* cDNA constructs on cell numbers and apoptosis, for the following reasons. Patient leukocytes show inclusions, similar to affected neurons in the brain. Lymphoblasts, as well as neurons, are susceptible to apoptosis. *CLN3*-overexpressing

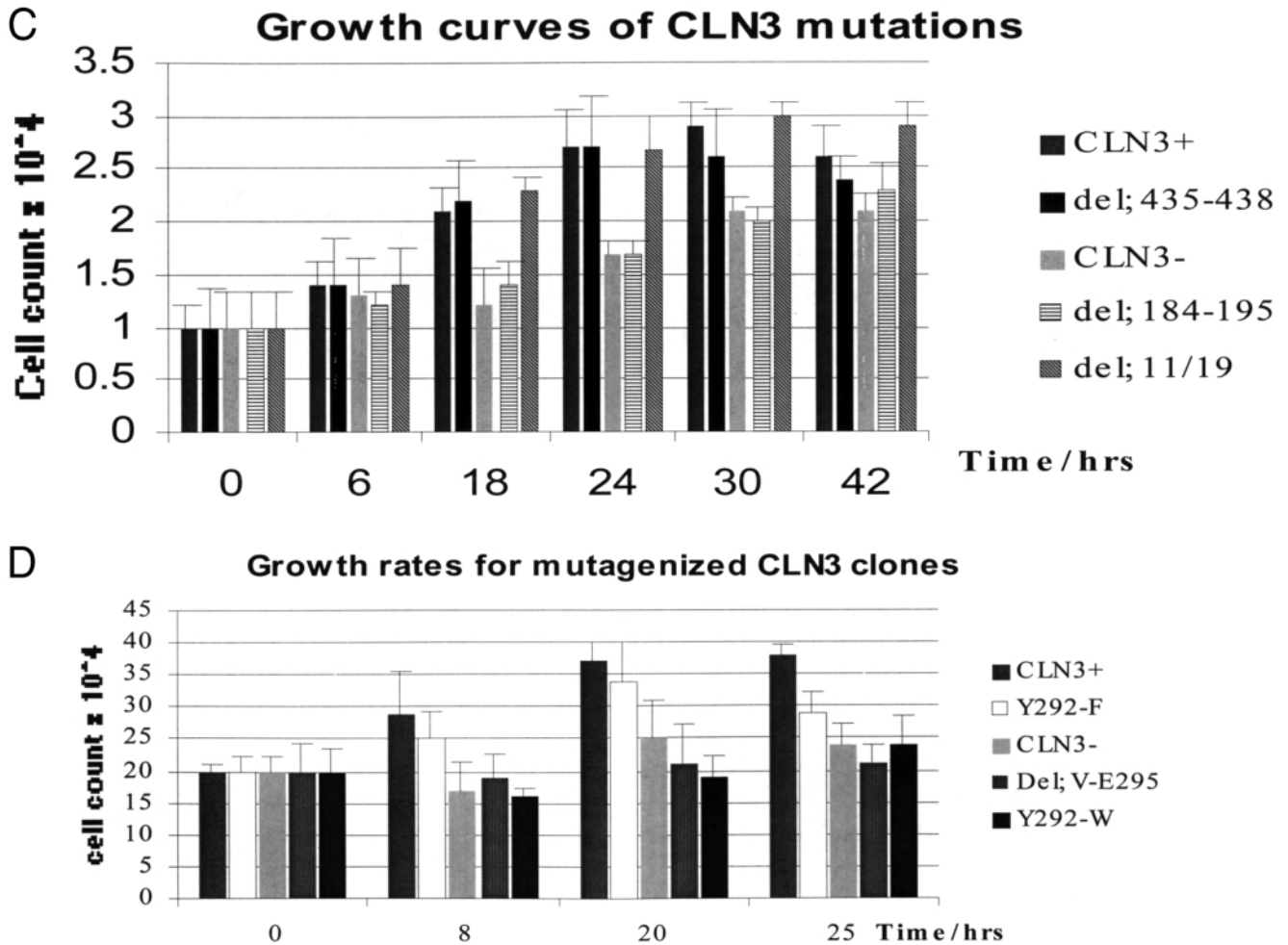


Figure 4 continued.

lymphoblasts show enhanced rates of growth, similar to CLN3-overexpressing neuron precursors. Lymphoblasts are easy to grow and maintain. Last, but not least, lymphoblasts derived from patients are abundantly accessible, unlike naturally deficient human neurons.

Immortalized CLN3-deficient lymphoblasts have provided a simple, reproducible and reliable model system for assessing the differential effect of a number of mutant *CLN3* constructs on cell growth rates and apoptosis. Growth curve analyses and JC-1 and TUNEL assays of JNCL patient lymphoblasts transfected with different *CLN3* constructs provided confirmation for the expected phenotypes of diminished growth and sensitivity to apoptosis (22,23,27). Expression of the CLN3 protein, confirmed by western blot, was shown to be similar for all *CLN3* cDNA constructs used and greater than expression with the empty vector control.

Previous studies have implicated CLN3 in cell growth and regulation pathways (28). Our results demonstrate that JNCL patient lymphoblasts have a slowed growth rate when compared to normal lymphoblasts. Transient transfection of intact *CLN3* cDNA into immortalized JNCL patient cells, with ensuing

production of CLN3 protein, completely reverses the growth defect. Western blot analysis shows that the mutated CLN3 protein's expression is not affected. The growth pattern is maintained while expression of the transfectant cDNA is present, but reverts back to deficient growth as expression of the CLN3p declines, as demonstrated by western blot. JNCL patient cells have a higher apoptotic rate than do normal cells. Again, introduction of the wild-type *CLN3* cDNA blocks apoptosis in JNCL patient cells.

The rates of thymidine incorporation into both wild-type and JNCL patient lymphoblast DNA are similar. However, growth analyses show that the respective cellular growth rates are statistically different. Results suggest that the CLN3 protein does not affect the rate at which the cell synthesizes DNA. The more likely scenario is that absence or mutation of the nascent CLN3 protein impacts on cell death pathways.

Previous studies have placed CLN3 upstream of ceramide in the mitochondria-dependent apoptotic cascade (22). Etoposide or VP-16 is a chemotherapeutic agent that inhibits topoisomerase II and induces mitochondria-dependent apoptosis (40–42). We demonstrate that JNCL patient cells show more protection from etoposide-induced apoptosis when transfected with full-

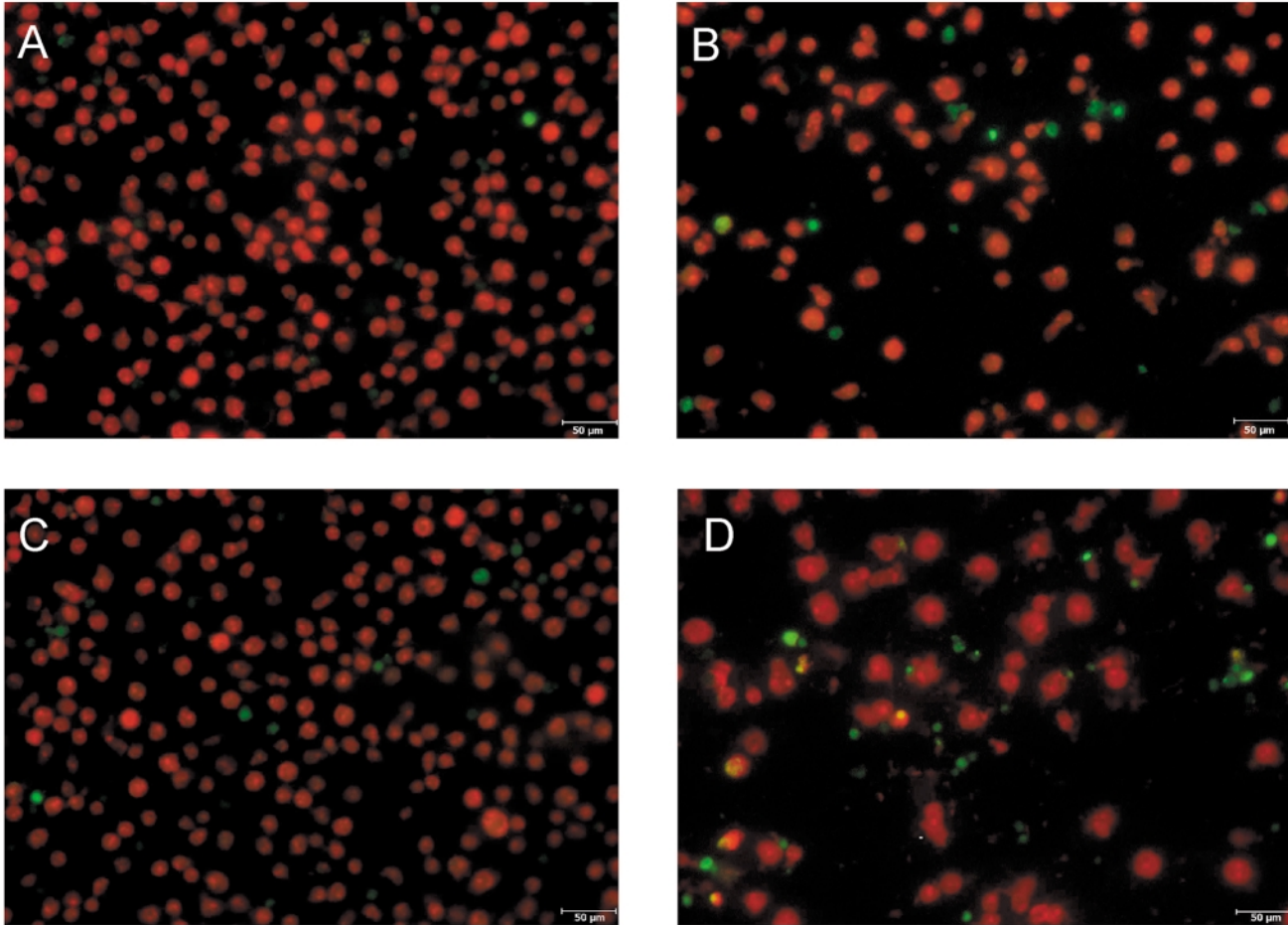


Figure 5. TUNEL staining of immortalized JNCL lymphoblasts transfected with CLN3 mutant constructs. (A, B) JNCL cells transfected with CLN3 mutant E295K. (C, D) JNCL lymphoblasts transfected with CLN3 mutant R334D. (A, C) JNCL cells before treatment with etoposide. (B, D) JNCL cells after treatment with etoposide. Live cells appear red, and cells undergoing apoptosis are green. These results are representative of mutations occurring at E295, V330 and R334. TUNEL staining shows that mutations at these sites result in increased apoptosis when compared to transfection with the wild-type CLN3 cDNA ($P < 0.05$). JC-1 results corroborate these data (data not shown). Magnification 400 \times , scale bar = 50 μm . CLN3 provides protection from etoposide-induced apoptotic death.

length CLN3 cDNA, as opposed to transfection with an empty vector control (96% versus 48%). This was determined by JC-1 and TUNEL assays. Expression of CLN3 protein, therefore, protects lymphoblasts from etoposide-induced apoptosis.

It is known that CLN3 has sequence-specific signals that can target the protein to individual organelles: a farnesylation site at residues 435CQLS438 (43) which anchors proteins to membranes, a mitochondrial targeting signal at residue 11 with its cleavage site at residue 19 (11), and a di-leucine lysosomal targeting motif at 424LL425 (17). The CLN3 protein is homologous across species for various motifs of potential biological relevance. These are the *N*-myristoylation site 2GGCAGS7, *N*-glycosylation sites 49NFSY52, 71NQSH74, 85NSSS88 and 310NTSL313, and the isoprenylation site 435CQLS438 (34). This indicates that CLN3 may be post-translationally modified in either the endoplasmic reticulum or the Golgi apparatus (17,19). Phosphorylation plays an important role in the targeting of proteins to membranes and can influence interactions with other proteins. Although there is evidence to suggest that CLN3 is phosphorylated (38), the independent deletion of each of the

phosphorylation sites does not affect cell growth rates in our assay system. Deletion of the sequences corresponding to the **CaaX** box within the CLN3 cDNA at residues 435–438 and the potential mitochondrial targeting signal did not have an effect on cell growth rates either. These results suggest but do not prove that CLN3 may be neither phosphorylated nor farnesylated, and nor is it targeted to the mitochondria. An alternative and more likely scenario is that post-translational modifications at the **CaaX** box and the phosphorylation sites do not determine the impact of the CLN3 protein on cell growth rates.

A CLN3 cDNA deletion strategy was designed to find which regions of the CLN3 protein contribute to the maintenance of cell growth rates and prevention of apoptosis in lymphoblasts. Sequences within exons 11 and 13 correspond to amino acid residues that are necessary for the CLN3 protein to negatively regulate apoptosis, and positively impact on cell growth rates. JNCL patient cells transfected with CLN3 deletion constructs missing exons 11 and 13 showed a growth potential similar to the one observed in JNCL patient or CLN3-deficient cells transfected with the empty vector. JC-1 analyses demonstrated

A Growth Rates for JNCL glycosylation mutants

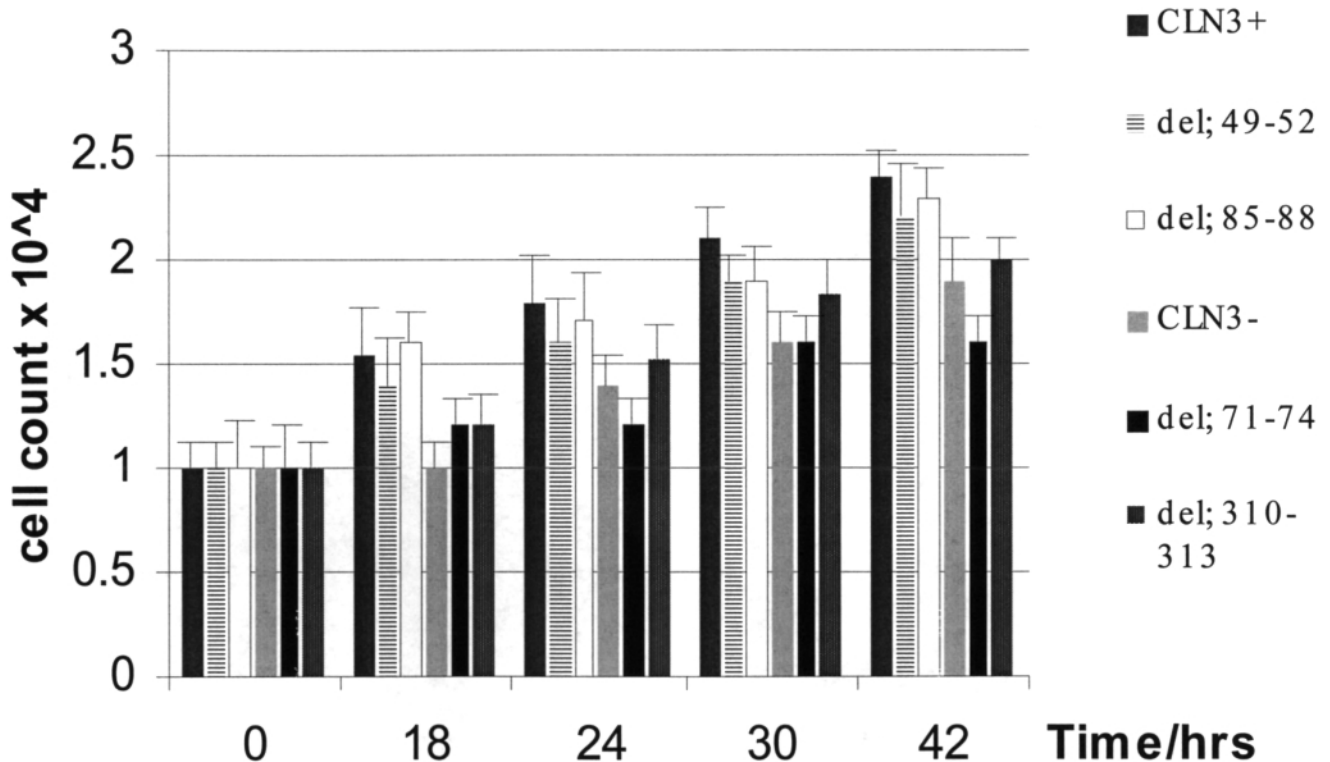


Figure 6. (A) Growth rates of JNCL lymphoblasts following transfection with CLN3 glycosylation mutant constructs. Deletion of the glycosylation sites at residues 71NQSH74 or 310NTSL313 maintains the observed growth defects following transfection of JNCL patient lymphoblasts, similar to the growth defect observed following transfection with the empty vector ($P > 0.05$). There is a marked decrease in the growth rate observed 25 h post-transfection. Mutations at sites 49–52 and 85–88 do not cause any growth defects when compared to normal CLN3 controls ($P > 0.5$, data not shown). The order of the transfected cell lines analyzed for each time point is indicated by the same sequence shown in the key on the right. (B) Hydropathy profile for CLN3 protein. The profile was generated at the website www.expasy.ch/tools/TMHMM and shows that CLN3 could have up to 11 transmembrane segments and a possible pore at residues 299–343. The glycosylation sites at residues 71NQSH74 and 310NTSL313 are indicated by stars and reside within the first external loop (L1), which is located between residues 61 and 98, and the putative pore region (P), which is between residues 299 and 343, respectively. Residues V330 and R334 are located within the putative pore (filled rectangles). The motif 291VYFAE295 is located within transmembrane segment 7 (filled triangle). Note: E295K, V330C and R334D are naturally occurring mutations.

that deletion of these regions had a corresponding effect on apoptosis.

CLN3 is a highly hydrophobic membrane-bound protein (11). The modeling algorithm used shows that CLN3 could harbor up to 11 transmembrane segments and a pore region. The generated hydropathy profile suggests that exon 11 forms part of putative transmembrane domain 7, and exon 13 forms part of the putative pore region. There are three residues within these exons that are highly conserved; they are E295 in exon 11, and V330 and R334 in exon 13.

Residue E295 is part of a highly conserved stretch of amino acids (VYFAE) found in CLN3 orthologs, K^+ channels (VYFAE) (35) and the amyloid- β precursor peptide (VFFAE) (36,37). The specific mutation E22K in the amyloid- β precursor protein has been shown to cause apoptosis in at least 30% of Alzheimer's patients (37). A similar mutation, E295K, is observed in JNCL patients (44). Decreased cell numbers and increased sensitivity to etoposide-induced apoptosis results

when the DNA sequence for this five amino acid stretch is deleted or when E295 is mutated to K295.

The mutation of tyrosine to phenylalanine at residue 292 (Y292F) does not have a significant effect on growth, but the change to tryptophan (Y292W) creates a growth phenotype similar to the one observed in JNCL patient cells. Phenylalanine (F) and tryptophan (W) are highly hydrophobic aromatic residues, in contrast to tyrosine (Y), which contains a hydroxyl group. Tryptophan is larger than phenylalanine. Both charge and size of the residue at position 292 in CLN3 could modulate the effect of the CLN3 protein on apoptosis and cell growth rates.

The naturally occurring mutations R334D, R334C and R334H (31) result in alteration of the charge of the amino acid from basic to acidic and produce a JNCL phenotype. The mutation R334K creates a similar charge, and therefore does not cause any significant growth defect. This suggests that the basic charge at R334 is of significance and needs to be

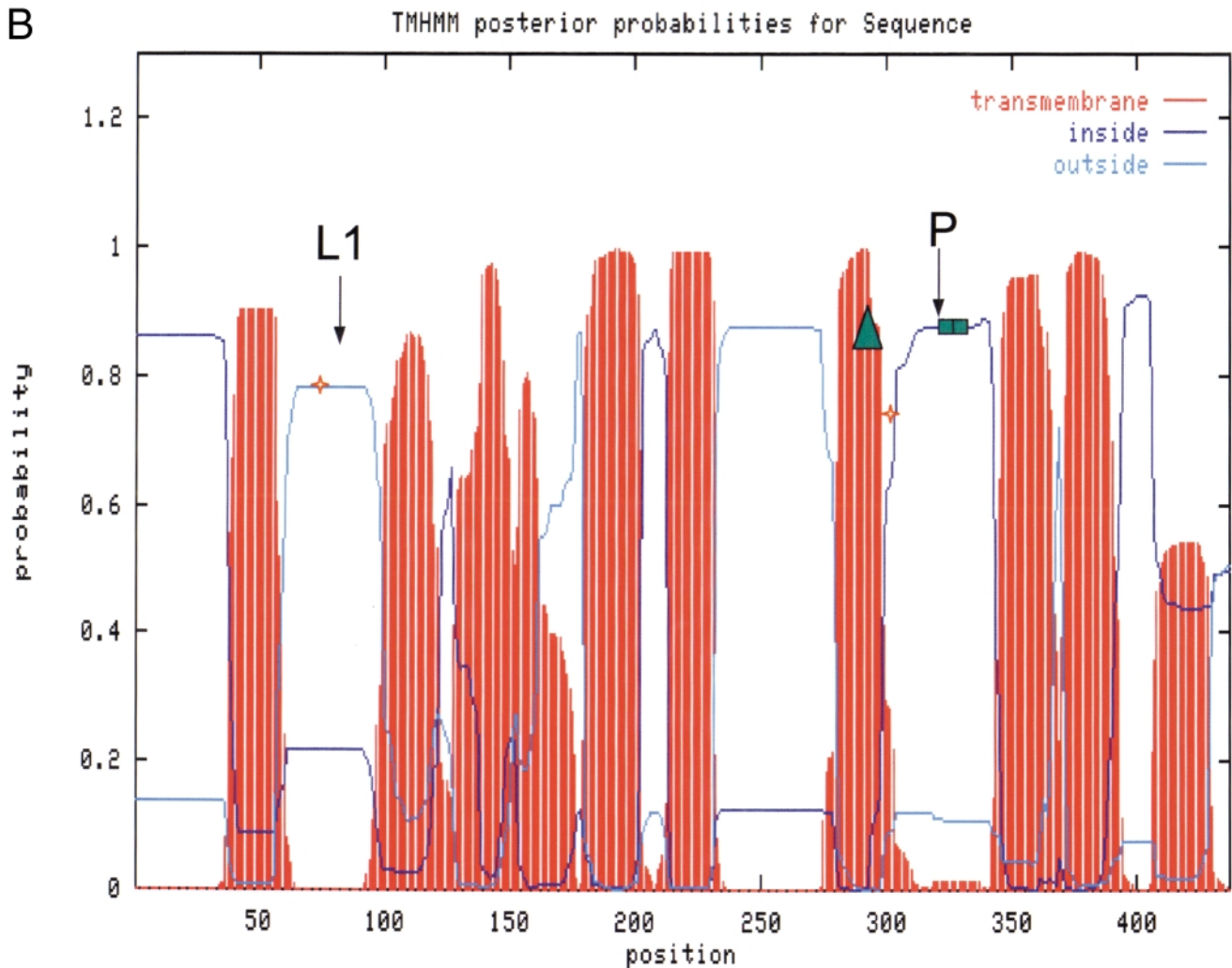


Figure 6 continued.

maintained for normal CLN3 impact on growth and apoptosis. The mutation at residue V330 has two major effects: it creates a growth phenotype similar to that observed for JNCL patient lymphoblasts, and also increases the sensitivity of cells to etoposide-induced apoptosis. Residues E295 and V330 are vital for preserving the effect of CLN3 on cell growth rates and apoptosis, but it is the charge and/or hydrophobicity at residue R334 that maintains these effects.

All these residues fall within the conserved amino acid stretches 291VYFAE295 and 330VFASRSSL337, suggesting these are two motifs within CLN3 are vital for safeguarding its normal modulation of cell growth rate and apoptosis.

CLN3 may be glycosylated, as two of the potential glycosylation sites at residues 71–74 and 310–313 are necessary for preservation of CLN3 impact on cell growth rates and apoptosis. According to the hydropathy profile, the glycosylation site at amino acid residues 71–74 resides within the putative first external loop (residues 61–98), and the glycosylation site at amino acid residues 310–313 is within the putative pore region (residues 299–343). These sites are in

locations that could be important for protein interactions. These could involve proteins deficient in other Batten variants, proteins that could interact with them, or proteins important for preserving CLN3 impact on cell growth rates. The effect of deleting residues 71–74 on the cell growth rate is worse than that of deleting residues 310–313. A possible explanation for this is that residues 71–74 are located within the first external loop of the CLN3 protein, a position that may be essential for targeting protein–protein and/or protein–lipid interactions. According to the presumed hydropathy profile presented in Figure 6B, residues 310–313 are internal. Glycosylation at these residues may be of no consequence; however, the location of these residues in the transmembrane segment bordering the putative pore may be important.

CONCLUSIONS

Additional data that substantiate the claim that the CLN3 protein impacts on apoptosis have been presented. The motif

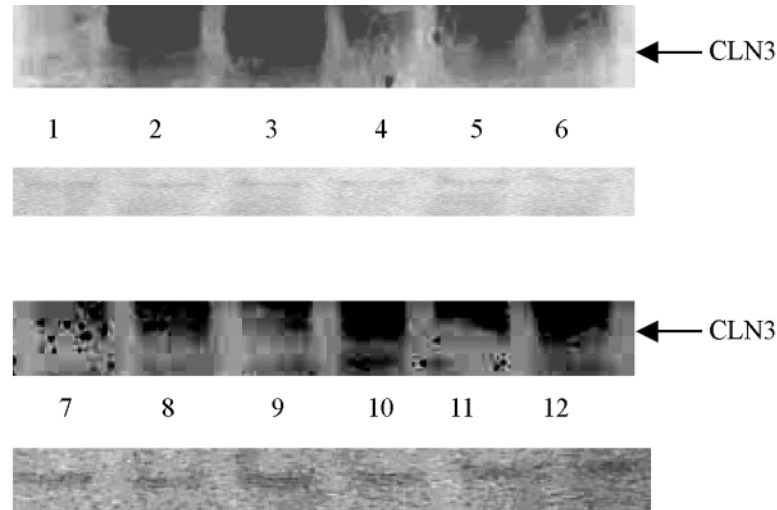


Figure 7. Western blot showing CLN3 protein expression following transfection with different *CLN3* constructs. CLN3 expression is indicated by the arrow (48 kDa). Lane 1 shows protein expression for JNCL lymphoblasts transfected with an empty vector control. Lane 2 is protein expression for JNCL lymphoblasts transfected with *CLN3* cDNA. Lane 3 is protein expression for wild-type lymphoblasts transfected with *CLN3* cDNA. Lanes 4–6 show protein expression for JNCL lymphoblasts transfected with the *CLN3* mutant constructs V330C, R334D and E295K respectively. Lane 7 is protein expression for wild-type lymphoblasts transfected with *CLN3* cDNA 50 h post-transfection. Lanes 8 and 9 show protein expression for immortalized wild-type lymphoblasts transfected with *CLN3* cDNA glycosylation site deletions at residues 71–74 and 310–313, respectively. Lanes 10 and 11 show protein expression for wild-type lymphoblasts transfected with *CLN3* cDNA deletion constructs containing exons 1–9 and 1–13, respectively. Lane 12 shows protein expression for immortalized wild-type lymphoblasts transfected with *CLN3* cDNA deletion of residues 291–295. To confirm equal protein loading, the nitrocellulose membrane was stained with Ponceau S stain (Sigma) and is shown below each lane.

291VYFAE295 appears to contribute to the preservation of this regulation and the positive modulating effect that CLN3 has on cell growth rates. Residues E295 and V330 also seem necessary for a CLN3 impact on cell growth rates and apoptosis. At site 334, it could be the charge of the residue that modulates this function. The potential glycosylation sites at residues 71–74 and 310–313 also appear to be important for the impact of CLN3 protein on cell growth rates. This indirectly supports previous claims that the CLN3 protein may be glycosylated.

According to the hydropathy profile, the glycosylation site 71NQSH74 resides within external loop 1, and the motif 291VYFAE295 and the potential glycosylation site 310NTSL313 line part of a putative pore region within transmembrane domain 7. Residues V330 and R334 are within the putative pore region. Will CLN3 turn out to be an ion pump, ion channel or transporter? Uncovering these amino acid motifs and knowledge of their contribution to the effects of the CLN3 protein on cell growth rates and apoptosis has narrowed specific molecular regions within this protein. These will facilitate the search for molecular partners of CLN3.

MATERIALS AND METHODS

Tissue culture

Lymphoblasts were grown in 24-well plates at $1\text{--}5 \times 10^4$ cells/ml per well at 37°C and in 5% CO_2 in RPMI 1640 media (Sigma, St Louis, MO, USA)/10% fetal bovine serum/1%

antibiotic–antimycotic/1× gentamicin. Immortalized lymphoblast cell lines, originally obtained from both JNCL patients and normal donors, were used for all experiments. These cell lines were established according to previously described methods (45). All JNCL patient lymphoblasts utilized are homozygous for the 1.02 kb deletion in the genomic DNA.

Trypan blue dye exclusion

Cells were harvested from 24-well plates by centrifugation at 1200 r.p.m. for 5 min and the supernatant was removed. Each pellet was resuspended in 1:1 mixture of 2% trypan blue dye (Gibco, Rockville, MD, USA) and 1× phosphate-buffered saline (PBS). Cells were loaded onto the hemocytometer and counted. Viable cells are white, and dead cells are blue. Live cell counts at each time point were performed in triplicate. The mean and standard deviation were calculated for each time point. Live cell counts were plotted for growth curves as live cell count $\times 10^4/\text{ml}$ against time. Live cell counts at each time point were then compared to those of transfection controls containing the full *CLN3* cDNA or an empty vector using Student's *t*-test to assess statistical significance.

Transfection of immortalized JNCL lymphoblasts

Cells, 8×10^5 , were plated in 24-well plates and incubated for 4–16 h at 37°C and in 5% CO_2 with *CLN3*–pGEM DNA–liposome complexes. The protocols according to those outlined for the Qiagen (Valencia, CA, USA) Effectene Transfection kit and the Lipofectamine 2000 (Invitrogen-Life Technologies, Carlsbad, CA, USA) were followed. The cells were then

washed and plated for analysis. The transfection efficiency was determined using the Clontech (Palo Alto, CA, USA) Luminescent β -galactosidase Detection Kit II. Transfected samples were compared to positive and negative controls. Light emission was then recorded by exposure to X-ray film or the Xenogen plate luminometer system. Transfection efficiencies in the range 90–95% were obtained ($P < 0.05$).

Cell proliferation/DNA synthesis assayed by thymidine incorporation

Cells, 5×10^4 , were plated as described previously and incubated with 0.2 μ l of 0.1 μ Ci/ μ l stock 3 H for 2 h at 37°C and in 5% CO₂. The cells were then washed twice with ice-cold PBS (Gibco-Invitrogen) and precipitated with 0.5% trichloroacetic acid on ice for 30 min. The cells were harvested and resuspended in 0.2 ml of 0.25% NaOH. The counts per minute (c.p.m.) were then measured using the Pharmacia scintillation counter (Pharmacia Corp. Peapack, NJ, USA). Cell counts/min at different time points were carried out in triplicate and the standard deviation was calculated. Statistical analysis was carried out using the Student's *t*-test.

Treatment with etoposide

Immortalized JNCL patient cells were transfected individually with the pGEM/*CLN3* construct or with an empty vector control. The cells were then harvested and incubated with 1 μ g/ml of etoposide (VP-16, Sigma) at 37°C and in 5% CO₂ for 18 h to induce apoptosis. The degree of protection from etoposide-induced apoptosis afforded by each construct was determined using the JC-1 assay. Comparisons were then made with transfected cells not treated with etoposide.

JC-1 analysis of mitochondrial membrane potential

JC-1 stain (5,5'-6'-tetrachloro-1,1,3,3-tetraethylbenzimidazolylcarbocyanine iodide; Molecular probes, Eugene, OR, USA) was used to assess the decrease in Ψ_m following treatment with etoposide. JC-1 is a cationic dye that forms J-aggregates with the cytochrome *c*-APAF-1 complex. Cells undergoing apoptosis are visualized when a shift in the emission spectrum from green (525 nm) to red (590 nm) occurs. This shift signals the onset of apoptosis. Immortalized lymphoblasts were grown in T-25 flasks at 5×10^5 in 5 ml of media and treated with etoposide as described above. The cells were then harvested, washed with 1 \times PBS and incubated with 1 μ g/ml of JC-1 stain for 15 min at 37°C and in 5% CO₂. The cells were again washed in PBS and then mounted on a slide with 1 : 1 PBS/glycerol mix. The cells in two different fields of vision were counted (60–200 cells/field) and the average numbers obtained. The degree of protection from etoposide-induced apoptosis was determined by dividing the percentage of live cells observed following treatment with etoposide by the percentage of live cells observed when not treated with etoposide. The statistical significance of the difference in the numbers of apoptotic cells (cells containing J aggregates appear yellow–red) between repeat experiments was determined by the two-tailed Student *t*-test.

TUNEL assay (terminal deoxynucleotide end labeling)

Sterile slides were treated overnight with poly(D) lysine (Sigma) and bordered off with a Super ht Pap pen (Research Products International Corp., Baltimore, MD, USA). Cells were plated and transfected as described previously. Cells, 1×10^4 , were placed onto the marked region of the treated slides and allowed to adhere. The TUNEL assay allows fragmented DNA, as is observed in apoptosis, to be end-labeled by a terminal transferase enzyme with digoxigenin. The APOALERT (Clontech) kit protocol was used. The cells were then viewed at 400 \times magnification with a LEICA fluorescent microscope. The cells in two different fields of vision were counted (60–200 cells/field) and the average numbers obtained. The degree of protection from etoposide-induced apoptosis was determined by the percentage of live cells treated with etoposide divided by the percentage of live cells not treated with etoposide. The statistical significance of the difference in the numbers of apoptotic cells between repeats was determined by the two-tailed Student *t*-test.

Deletion construct generation

The *CLN3* cDNA was cloned into the pGEM (+)7f(–) plasmid (Promega, Madison, WI, USA). *CLN3*/pGEM (+)7f(–), 10 μ g, was double digested with 10–20 U each of the restriction enzymes *Sac*I (*Exo*III susceptible) and *Bam*HI (*Exo*III resistant) (New England Biolabs, Beverly, MA, USA) overnight at 37°C. The appropriate bands were then cut out of a 1% agarose gel. The linearized plasmid was then digested with *Exo*III nuclease according to the Promega Erase-a-Base Kit protocol. A constant temperature of 25°C was maintained to enable accurate digestion by the exonuclease (90 base/min). The desired fragments were then individually ligated and cloned into supercompetent bacterial cells (Stratagene, La Jolla, CA, USA). Each clone was then sequenced by automated sequencing to verify that the required exons are present. These were plated for cell transfections and growth curve analysis.

Western blot

Western blot analysis was performed as previously described (22). Cells were transfected with different *CLN3* cDNA constructs (described above) and harvested in lysis buffer as previously described (27). Cells were harvested at maximum *CLN3*p expression, 48 h post-transfection.

Site-directed mutagenesis

The Stratagene Quikchange Site-Directed Mutagenesis kit protocol was used to introduce the desired mutations in the *CLN3* cDNA. The PCR cycles used were as per the protocol: 12 cycles for point mutations; 16 cycles for single amino acid changes; and 18 cycles for multiple amino acid deletion/insertion. JNCL mutations include: V330C, V330L, R334D, R334K, R334C, R334H, E295K, E295D, Δ V291–E295, Y292F, Y292W and Δ I84WSSGTGGAGLLG195. Phosphorylation mutations include deletions of the DNA sequences for amino acid residues 7, 12, 14, 19, 64, 73, 86, 125, 232, 270, 336 and 400. Glycosylation mutations include

deletion of residues 49–52, 71–74, 85–88 and 310–313. The mitochondrial targeting signal mutation involved the deletion of residue 11. The isoprenylation site mutation involved the deletion of residues 435–438. Primers were made to incorporate these changes, with the mutations residing in the middle of normal *CLN3* flanking sequence. All primers are 24–30 nucleotides in length.

ACKNOWLEDGEMENTS

The authors wish to thank the Batten Diseases Support and Research Association for their generous support. This work was carried out in part with support from 3 RO1 NS30170-08S1 (R.-M.B.), and the Duke University Genetics Training Grant 5T32GM07754 (D.P.S.).

REFERENCES

- Zhong, N. (2000) Neuronal ceroid lipofuscinoses and possible pathogenic mechanism. *Mol. Gen. Met.*, **71**, 195–206.
- The International Batten Consortium (1995) Isolation of a novel gene underlying Batten disease, *CLN3*. *Cell*, **82**, 949–957.
- Boustany, R.-M. (1996) Batten disease or neuronal ceroid lipofuscinosis. In Vinken, P.J., Bruyn, G.W. and Moser, H.W. (eds), *Handbook of Clinical Neurology, Neurodystrophies and Neurolipidoses*. Vol. **66**, Elsevier Sciences, New York, pp. 671–900.
- Goebel, H.H. (1997) Morphologic diagnosis in neuronal ceroid lipofuscinoses. *Neuropediatrics*, **28**, 67–69.
- Schmechel, D.E. (1999) Apoptosis in neurodegenerative disorders. In Hannun, Y. and Boustany, R.-M. (eds), *Apoptosis in Neurobiology*. CRS Press, Boca Raton, FL, pp. 29–30.
- Kida, E., Golabek, A. and Wisniewski, K.E. (2001) Cellular pathology and pathogenic aspects of neuronal ceroid lipofuscinoses. *Adv. Genet.*, **45**, 35–68.
- Johnson, D.W., Speier, S., Qian, W.-H., Lane, S., Cook, A., Suzuki, K., Daniel, P. and Boustany R.-M. (1995) Role of subunit 9 of mitochondrial ATP synthase in Batten disease. *Am. J. Med. Genet.*, **57**, 350–360.
- Pullarkat, R.K., Kim, K.S., Sklower, S.L. and Patel, V.K. (1998) Oligosaccharyl diphosphodolichols in the ceroid-lipofuscinoses. *Am. J. Med. Genet. suppl.* **5**, 243–251.
- Sleat, D.E., Donnelly, R.J., Lackland, H., Liu, C.G., Sohar, I., Pullarkat, R.K. and Lobel, P.S. (1997) Association of mutations in a lysosomal protein with classical late-infantile neuronal ceroid lipofuscinosis. *Science*, **277**, 5333, 1802–1805.
- Vesa, J., Hellsten, E., Verkruyse, L.A., Camp, L.A., Rapola, J., Santavuori, P., Hofmann, S.L. and Peltonen, L. (1995) Mutations in the palmitoyl protein thioesterase gene causing infantile neuronal ceroid lipofuscinosis. *Nature*, **376**, 584–587.
- Janes, R.W., Munroe, P.B., Mitchison, H.A., Gardiner, R.M., Mole, S.E. and Wallace, B.A. (1996) A model for Batten disease protein *CLN3*: functional implications from homology and mutations. *FEBS Lett.*, **399**, 75–77.
- Savukoski, M., Klockars, T., Holmberg, V., Santavuori, P., Lander, E.S. and Peltonen, L. (1998) *CLN5*, a novel gene encoding a putative transmembrane protein mutated in Finnish variant late infantile neuronal ceroid lipofuscinosis. *Nat. Genet.*, **19**, 286–288.
- Gao, H., Boustany, R.-M., Espinola, J.A., Cotman, S., Srinidhi, L., Antonellis, K.A., Gillis, T., Stout, D., Haines, J.L., Lerner, T.J. and MacDonald, M.E. (2002) Mutations in a novel *CLN6* encoded transmembrane protein cause variant neuronal ceroid lipofuscinosis in mouse and man. *Am. J. Hum. Genet.*, **70**, 324–335.
- Ranta, S., Zhang, Y., Ross, B., Lonka, L., Takkunen, E., Messer, A., Sharp, J., Wheeler, R., Kusumi, K., Mole, S.E. *et al.* (1999) The neuronal ceroid lipofuscinoses in human EPMR and *mnd* mutant mice are associated with mutations in *CLN8*. *Nat. Genet.*, **23**, 233–236.
- Margraf, L.R., Boriack, R.L., Routheut, A.A., Cuppen, I., Alhilali, L., Bennett, C.J. and Bennett, M.J. (1999) Tissue expression and subcellular localization of *CLN3*, the Batten disease protein. *Mol. Gen. Met.*, **66**, 283–289.
- Haskell, R.E., Carr, C.J., Pearce, D., Bennett, M.J. and Davidson B.L. (2000) Batten disease: evaluation of *CLN3* mutations on protein localization and function. *Hum. Mol. Genet.*, **9**, 735–744.
- Jarvela, I., Sainio, M., Rantmaki, T., Olkkonen, V.M., Carpen, O., Peltonen, L. and Janes, R.W. (1998) Biosynthesis and intracellular targeting of the *CLN3* protein defective in Batten disease. *Hum. Mol. Genet.*, **7**, 265–271.
- Katz, M.L., Gao, C.-L., Prabhakaram, M., Shibuya, H., Liu, P.-C. and Johnson, G.S. (1997) Immunohistochemical localization of the Batten disease (*CLN3*) protein in retina. *Invest Ophthalmol Vis. Sci.*, **38**, 2375–2386.
- Kremmidiotis, G., Lensink, I., Bilton, R.L., Woolatt, E., Chataway, T.K., Sutherland, G.R. and Callen, D.F. (1999) The Batten disease gene product (*CLN3p*) is a Golgi integral membrane protein. *Hum. Mol. Genet.*, **8**, 523–531.
- Jarvela, I., Lehtovirta, M., Tikkanen, R., Kytala, A. and Jalanko, A. (1999) Defective intracellular transport of *CLN3* is the molecular basis of Batten disease. *Hum. Mol. Genet.*, **8**, 1091–1098.
- Luiro, K., Kopra, O., Lehtovirta, M. and Jalanko, A. (2001) *CLN3* protein is targeted to neural synapses but excluded from synaptic vesicles: new clues to Batten disease. *Hum. Mol. Genet.*, **10**(19), 2123–2131.
- Puranam, K.L., Guo, W.-X., Qian, W.-H., Nikbakht, K. and Boustany, R.-M. (1999) *CLN3* defines a novel antiapoptotic pathway operative in neurodegeneration and mediated by ceramide. *Mol. Gen. Met.*, **66**, 294–308.
- Dhar, S., Bitting, R.L., Rylova, S., Jansen, P.J., Lockhart, E., Koeberl, D.D., Amalfitano, A. and Boustany, R.-M. (2001) Flupirtine blocks apoptosis in Batten patient lymphoblasts and in human post-mitotic *CLN3*- and *CLN2*-deficient neurons. *Ann. Neurol.*, **51**, 448–466.
- Lane, S.C., Jolly, R.D., Schmechel, D.E., Alroy, J. and Boustany, R.-M. (1996) Apoptosis as the mechanism of neurodegeneration in Batten's disease. *J. Neurochem.*, **67**, 677–683.
- Kieser, B.C., Wisniewski, K.E., Park, E., Schiller-Levis, G., Mehta, P.D. and Goebel, H.H. (1997) Leukocytes in neuronal ceroid lipofuscinoses; function and apoptosis. *Brain Dev.*, **19**, 317–322.
- Pane, M.A., Puranam, L. and Boustany, R.-M. (1999) Expression of *cln3* in human NT2 neuronal precursor cells and neonatal rat brain. *Pediatr. Res.*, **46**, 367–374.
- Rylova, S.N., Amalfitano, A., Persaud-Sawin, D.A., Guo, W.-X., Chang, J., Jansen, P.J., Proia, A.D. and Boustany, R.-M. (2002) The *CLN3* gene is a novel molecular target for cancer drug discovery. *Cancer Res.*, **62**, 801–808.
- Guo, W.-X., Mao, C., Obeid, L. and Boustany, R.-M. (1999) A disrupted homolog of the *CLN3* or Juvenile Neuronal Ceroid Lipofuscinosis gene in *Saccharomyces cerevisiae*. *Cell. Mol. Neurol.*, **19**, 671–680.
- Pearce, D.A., Ferea, T., Nosel, S.A., Das, B. and Sherman, F. (1998) Action of *BTN1*, the yeast ortholog of the gene mutated in Batten disease. *Nat. Genet.*, **22**, 55–58.
- Matsuyama, S., Llopis, J., Devereaux, Q.L., Tsien, R.Y. and Reed, J.C. (2000) Changes in intramitochondrial and cytosolic pH: early events that modulate caspase activation during apoptosis. *Nat. Cell Biol.*, **28**, 18–20.
- Mole, S.E., Mitchison, H.A. and Munroe, P.B. (1999) Molecular basis of the neuronal ceroid lipofuscinoses: mutations in *CLN1*, *CLN2*, *CLN3* and *CLN5*. *Hum. Mut.*, **14**, 199–215.
- Mole, S.E., Zhong, N., Saprong, A., Logan, W.P., Hofmann, S.L., Zhong, N., Franken, P.F., Van Diggelen, O.P., Bruening, M.H., Moroziewicz, D.N. *et al.* (2001) New mutations in the neuronal ceroid lipofuscinosis genes. *Eur. J. Pediatr. Neurol.*, **5**, 7–10.
- Munroe, P.B., Mitchison, H.A., O'Rawe, A.M., Anderson, J.W., Boustany, R.-M., Lerner, T.J., Taschner, P.E.M., de Vos, N., Bruening, M.H., Gardiner, R.M. and Mole, S.E. (1997) Spectrum of mutations in the Batten disease gene, *CLN3*. *Am. J. Hum. Genet.*, **61**, 310–316.
- Taschner, P.E.M., de Vos, N. and Bruening, M.H. (1997) Cross-species homology of the *CLN3* gene. *Neuropediatrics*, **28**, 18–20.
- Kerr, I.D., Ranatunga, M.K. and Sansom, M.S.P. (1999) The voltage gated potassium channel: sequence analysis and pore modeling of the pore domain. *Perspect. Drug Disc. Des.*, **15/16**, 187–214.
- Gelbard, H.A., Boustany, R.-M. and Schor, N.F. (1997) Apoptosis in development and disease of the nervous system: II. Apoptosis in childhood neurologic disease. *Pediatr. Neurol.*, **16**, 93–97.
- Miravalle, L., Tokuda, T., Chiarle, R., Giaccone, G., Bugiani, O., Tagliavini, F., Frangione, B. and Ghiso, J. (2000) Substitution at codon 22 of the Alzheimer's A-beta peptide induces conformational changes and apoptotic effects in the human cerebral endothelial cells. *J. Biol. Chem.*, **275**, 27110–27116.

38. Michalewski, M.P., Kaczmarek, W., Golabek, A., Kida, E., Kaczmarek, A.L. and Wisniewski, K.E. (1998) Evidence for phosphorylation of CLN3 protein associated with Batten disease. *Biochem. Biophys. Res. Commun.*, **253**, 458–462.
39. Michalewski, M.P., Kaczmarek, W., Golabek, A., Kida, E., Kaczmarek, A.L. and Wisniewski, K.E. (1999) Posttranslational modification of CLN3 protein and its possible functional implication. *Mol. Gen. Met.*, **66**, 272–276.
40. Facompre, M., Watzel, N., Kluza, J., Lansiaux, A. and Bailly, C. (2000) Relationship between cell cycle changes and variations of the mitochondrial membrane potential induced by etoposide. *Mol. Cell Biol. Res. Commun.*, **4**, 37–42.
41. Sawada, M., Nakashima, S., Banno, Y., Kamakawa, H., Hayashi, K., Tanaka, K., Nishimura, Y., Saki, N. and Nozawa, Y. (2000) Ordering of ceramide activation and Bax/Bcl-2 expression during etoposide induced apoptosis in C6 glioma cells. *Cell Death Diff.*, **7**, 761–772.
42. Cervinka, M., Bereiter-Hahn, J., Peychl, J., Rudolf, E. and Cervinkova, Z. (1999) The role of the mitochondria in apoptosis induced *in vitro*. *Gen. Phys. Biophys.*, **18**, 33–40.
43. Pullarkat, R.K. and Morris, G.N. (1997) Farnesylation of Batten disease CLN3 protein. *Neuropediatrics*, **28**, 42–44.
44. Zhong, N., Wisniewski, K.E., Kaczmarek, A.L., Ju, W., Xu, W.M., Xu, W.W., Melendon, L., Liu, B., Kaczmarek, W., Brooks, S.S. and Brown, W.T. (1998) Molecular screening of Batten disease: identification of a mis-sense mutation (E295K) in the CLN3 gene. *Hum. Genet.*, **102**, 57–62.
45. Anderson, M.A. and Gusella, J.F. (1984) Use of cyclosporine A in establishing Epstein–Barr virus-transformed human lymphoblastoid cell lines. *In Vitro*, **20**, 856–858.